ORIGINAL RESEARCH

Velocity Pulsatility and Arterial Distensibility Along the Internal Carotid Artery

Rick J. van Tuijl (ID), MSc; Ynte M. Ruigrok, MD, PhD; Birgitta K. Velthuis, MD, PhD; Irene C. van der Schaaf, MD, PhD; Gabriël J. E. Rinkel, MD, PhD; Jaco J. M. Zwanenburg (ID), PhD

BACKGROUND: Attenuation of velocity pulsatility along the internal carotid artery (ICA) is deemed necessary to protect the microvasculature of the brain. The role of the carotid siphon within the whole ICA trajectory in pulsatility attenuation is still poorly understood. This study aims to assess arterial variances in velocity pulsatility and distensibility over the whole ICA trajectory, including effects of age and sex.

METHODS AND RESULTS: We assessed arterial velocity pulsatility and distensibility using flow-sensitized 2-dimensional phase-contrast 3.0 Tesla magnetic resonance imaging in 118 healthy participants. Velocity pulsatility index ($vPI=(V_{max}-V_{min})/V_{mean}$) and arterial distensibility defined as area pulsatility index ($(A_{max}-A_{min})/A_{mean}$) were calculated at C1, C3, and C7 segments of the ICA. vPI increased between C1 and C3 (0.85 ± 0.13 versus 0.93 ± 0.13, $P<0.001$ for averaged right+left ICA) and decreased between C3 and C7 (0.93 ± 0.13 versus 0.84 ± 0.13, $P<0.001$) with overall no effect (C1–C7). Conversely, the area pulsatility index decreased between C1 and C3 (0.18 ± 0.06 versus 0.14 ± 0.04, $P<0.001$) and increased between C3 and C7 (0.14 ± 0.04 versus 0.31 ± 0.09, $P<0.001$). vPI in men is higher than in women and increases with age ($P<0.015$). vPI over the carotid siphon declined with age but remained stable over the whole ICA trajectory.

CONCLUSIONS: Along the whole ICA trajectory, vPI increased from extracranial C1 up to the carotid siphon C3 with overall no effect on vPI between extracranial C1 and intracranial C7 segments. This suggests that the bony carotid canal locally limits the arterial distensibility of the ICA, increasing the vPI at C3 which is consequently decreased again over the carotid siphon. In addition, vPI in men is higher and increases with age.

Key Words: cerebral hemodynamics ■ distensibility ■ internal carotid artery ■ MRI angiography ■ velocity pulsatility index

Decrease in velocity pulsatility along the internal carotid artery (ICA) is deemed necessary to protect the microvasculature of the brain against excessive pulse pressures.[1] The ability of arteries to decrease pulsatility can be hindered by different conditions, such as stiffening of the arterial wall, atherosclerosis, and hypertension.[2–4] Increased pulsatility is associated with cardiovascular disease, stroke, and vascular dementia because of damage to the microcirculation,[5] and may also be associated with the presence of intracranial aneurysms.[6]

Several studies have characterized arterial flow waveforms of the ICA in health and disease.[7–10] Most of these studies provided detailed qualitative and quantitative analysis of the normal arterial flow waveform. The siphon of the ICA is known to attenuate arterial flow pulsation.[11] However, our understanding of the role of the carotid siphon in decreasing velocity pulsatility over the ICA is still limited, as little is known about the relationship between velocity pulsatility and arterial distensibility along the whole ICA trajectory, including its extracranial—and intracranial parts. In addition, the influence of age and sex on pulsatility variation and arterial distensibility over the entire ICA is not known.

This study aims to (1) assess velocity pulsatility and arterial distensibility of the ICA by measuring the lumen

CLINICAL PERSPECTIVE

What Is New?

- Internal carotid artery velocity pulsatility is variable along the internal carotid artery and is inversely related to the area pulsatility (wall distensibility).
- Distensibility is constrained by the bony carotid canal segment of the internal carotid artery, thus increasing the pulsatility.
- Velocity pulsatility increases with age, and is higher in men than in women.

What Are the Clinical Implications?

- If velocity pulsatility is used as a metric for vascular health, care should be taken to relate measurements to location, subject sex, and age.
- Velocity pulsatility is not only affected by upstream arterial elasticity or downstream (micro) vascular resistance, but also by local constraints to arterial vessel distensibility, such as the bony carotid canal and possibly (calcified) atherosclerotic lesions.

Nonstandard Abbreviations and Acronyms

aPI	area pulsatility index
BA	basilar artery
ERASE	Early Recognition of Persons at High Risk of Aneurysmal Subarachnoid Hemorrhage
fPI	flow pulsatility index
ICA	internal carotid artery
PCA	phase contrast angiography
PC-MRI	phase contrast (velocity) magnetic resonance imaging
ROI	region of interest
vPI	velocity pulsatility index

area pulsatility at 3 segments of the ICA, covering both extracranial—and intracranial parts, and (2) test the influence of age and sex on variation in velocity pulsatility and arterial distensibility over the ICA.

MATERIALS AND METHODS

Data Availability

Anonymized data will be shared upon reasonable request to the corresponding author.

Subjects

Data were obtained from subjects from the ongoing ERASE (Early Recognition of Persons at High Risk of Aneurysmal Subarachnoid Hemorrhage) study using 3.0 Tesla magnetic resonance imaging (MRI) at the University Medical Center Utrecht from June 2017 until October 2019. The objective of the ERASE study is to determine the prevalence of unruptured intracranial aneurysms in people with ≥1 first-degree relative(s) with an unruptured intracranial aneurysm. The local ethics review committee approved the study and written informed consent was obtained from all subjects.

MRI Acquisition

As part of the ERASE study protocol, subjects were scanned on a 3.0 Tesla MRI with a 32-channel head coil (Philips, Best, The Netherlands). Coronal and sagittal phase-contrast angiography (PCA) surveys were made first to plan a time-of-flight magnetic resonance angiography. The PCA localizers and time-of-flight magnetic resonance angiography were used to identify the 3 vessels; right ICA, left ICA, and basilar artery (BA). Subsequently, 2-dimensional (2D) phase-contrast magnetic resonance imaging (PC-MRI) acquisitions were used to acquire time-resolved measurements of blood velocities and volumetric flow rates at 3 different segments planned on both the PCA and time-of-flight magnetic resonance angiography images. The classification of Bouthillier[12] was used for slice planning of C1 (extracranial ICA), C3 (ICA in the bony carotid canal proximal to the carotid siphon), and C7 (terminal intracranial part of the ICA). The planning is illustrated in Figure 1. The first 144 patients were scanned with a single 2D PC-MRI acquisition plane to include both ICAs at the C7 segment, conform C1 and C3 segment. As the ICAs were found to diverge slightly at C7 segment, the last 58 patients underwent separate 2D PC-MRI acquisitions for each C7 segment. The 2D PC acquisitions were performed with a 2D radiofrequency-spoiled gradient-echo sequence with retrospective cardiac gating (using a pulse pressure unit on the tip of the finger) and unidirectional through-plane velocity encoding with the following imaging parameters (ranges: depending on slice angulation): 250×250 mm field of view, acquired spatial resolution $0.5×0.5×3.0$ mm^3, reconstructed resolution $0.25×0.25×3.0$ mm^3, TR/TE=6.6 to 7.2/3.3 to 3.5 ms, flip angle=50°, bandwidth=467 to 522 Hz/pixel and acquired temporal resolution of 66 to 71.9 ms. Velocity encoding sensitivity was 90 cm/s for C1 and C3, and 150 cm/s for C7 segments. The acquisition time was ≈51 seconds for a heart rate of 60 bpm, and 100% scan efficiency (no
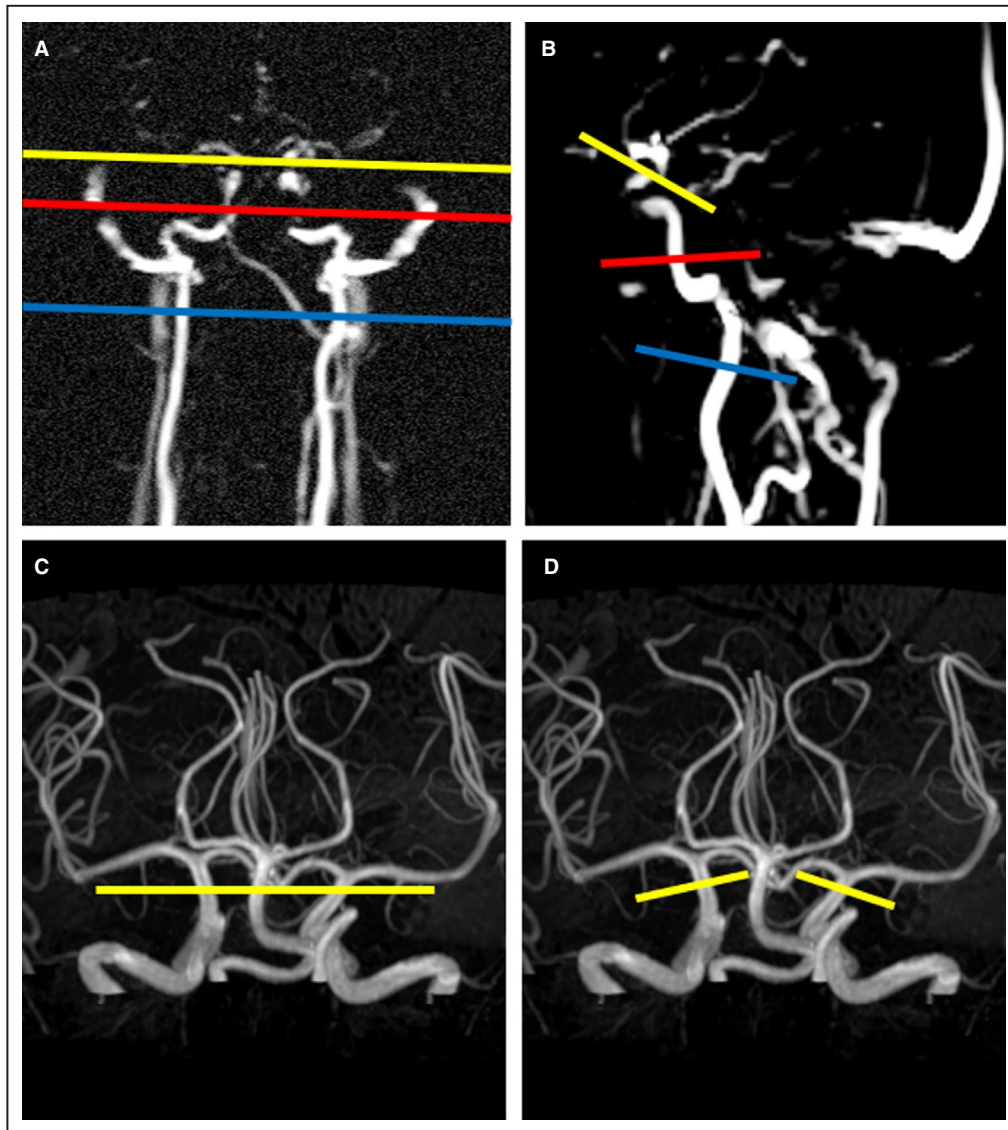
Figure 1. Planning of the 2D phase contrast velocity measurements on different segments of the internal carotid artery.

A and **B**, Coronal and sagittal oriented phase contrast angiography surveys used to plan the 2D phase contrast velocity measurements at C1 (blue line) and C3 (red) segments. The planning of the C7 (yellow) segment is also illustrated in the phase contrast angiography surveys. Planning of the C7 segment was fine-tuned using a maximum intensity projection of the 3D time-of-flight angiogram (**C** and **D**). **C**, Until February 2019, a single 2D phase-contrast measurement was used for simultaneous assessment of both right and left internal carotid artery. **D**, From February 2019 until October 2019, the phase-contrast velocity measurements of the right and left internal carotid artery at C7 segments were planned separately to compensate for the slightly diverging angle at C7 level.

detected arrhythmias). The 2D PC-flow acquisitions resulted in a series of 2D images, representing the blood-flow velocity and arterial distensibility can be measured in consecutive timeframes of the cardiac cycle as shown in Figure 2 for a representative subject. Subjects included until February 2019 received a single 2D PCA acquisition at the C7 segment, which, upon analysis, appeared suboptimal as often only 1 ICA C7 segments was perpendicular to the

acquisition plane. Subjects scanned after February 2019 received separate acquisitions for the left and right ICA at C7.

Subjects were excluded if they had undergone carotid or vertebrobasilar surgical or endovascular treatment. The remaining subjects were eligible if they had complete 3.0 Tesla MRI data sets containing flow measurements for all 3 segments of the ICA. Flow measurements were evaluated per
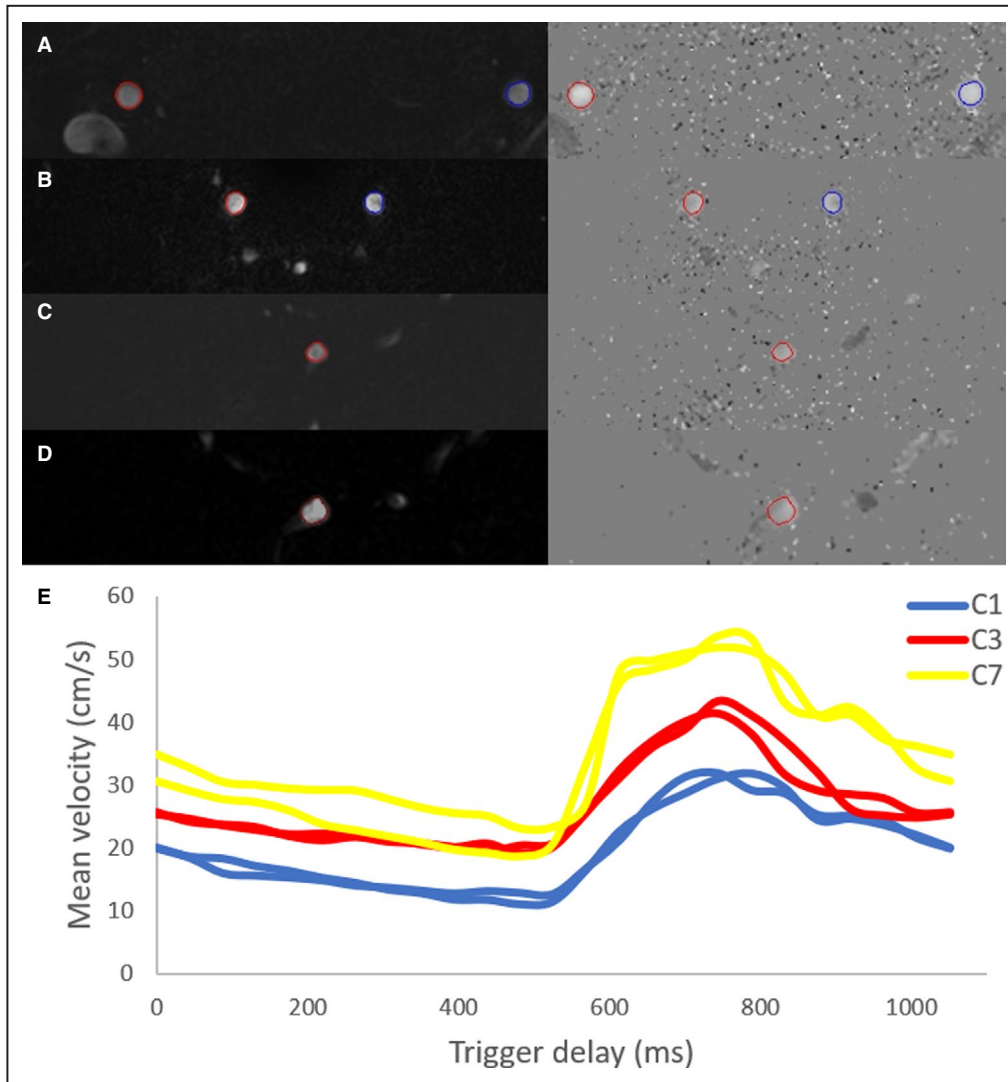
Figure 2. Magnitude and phase contrast images shown for 3 different segments for the first heart phase within 1 representative subject.
For every segment the contour (region of interest) was automatically drawn and propagated. All regions of interest were included for this representative subject. **A**, segment C1. **B**, segment C3. **C**, segment C7 right. **D**, segment C7 left. **E**, All mean velocity curves (in cm/s) of this subject are combined and shown over trigger delay (in milliseconds) for the 3 segments, C1 (blue), C3 (red) and C7 (yellow) of the internal carotid artery.

segment (C1, C3, and C7) and per vessel (right ICA, left ICA and BA). The BA was included as reference for variation in velocity pulsatility and arterial distensibility along a straight vessel segment. The measurements of a subject were included if all of the following quality criteria were met for all segments of at least 1 vessel: (1) the image slice is planned perpendicular to the vessel, meaning that the contour is circular and regular for all 3 segments over all heart phases. (2) The contour is stable with only minor region of interest (ROI) variation between heart phases for every segment, and (3) the contour of the region of interest follows the vessel contour for every segment.

Data Processing

Semi-automated analysis of the 2D PC acquisitions was performed by 1 researcher (RvT) on a standalone workstation using the software of the scanner console (Philips, software release R5.1.7). Contours were automatically created and propagated for the entire cardiac cycle after a single mouse click in the respective vessel for every segment. This propagation (with "active contours") over cardiac cycles enabled extraction of variation in blood flow, velocity, and vessel area, as well as the stroke volume. The results, consisting of velocity curves, area curves, and volume flow curves (all time resolved), were exported as comma-separated values files.

The minimum, maximum, and mean blood volume velocities (V_{min}, V_{max} and V_{mean}) in (cm/s), were used to calculate the velocity pulsatility index (vPI) from each velocity curve[13]:

$$vPI = \frac{V_{max} - V_{min}}{V_{mean}} \quad (1)$$

Similarly, area pulsatility index (aPI) was calculated from the minimum, maximum, and mean areas (ROI_{min}, ROI_{max} and ROI_{mean}) from each area curve:

$$aPI = \frac{ROI_{max} - ROI_{min}}{ROI_{mean}} \quad (2)$$

Finally, the flow pulsatility index (fPI),was calculated from the minimum, maximum, and mean blood volume flow rates (F_{min}, F_{max}, and F_{mean}) in (mL/s) from each volume flow curve:

$$fPI = \frac{F_{max} - F_{min}}{F_{mean}} \quad (3)$$

The pulsatility indices vPI, aPI, and fPI were directly calculated in Excel (Microsoft) from the exported text files, and the results of all subjects were combined and transferred to IBM Statistics Package for Social Sciences (SPSS) Version 25 (Chicago, IL, USA) for statistical analysis.

Statistical Analysis

We assessed differences in vPI, aPI, and fPI in all subjects between the extracranial C1 and carotid canal C3, carotid canal C3 and intracranial C7, and extracranial C1 and intracranial C7 for both the right ICA and left ICA and between C3 and C7 segment for the BA (used as reference for the behavior of a straight vessel without the constraints of a bony canal) using paired t tests. All statistical analyses were performed for vPI, aPI, and fPI, although vPI was used as the primary outcome because fPI is directly dependent on aPI and vPI (flow=velocity×area). A paired t test was also used to compare differences in velocity (V_{mean} and V_{max}) between all segments. To assess the influence of age and sex on vPI and aPI between the 3 segments, we used a linear mixed-effects model with the segment as mixed-effect for vPI and aPI. The linear mixed-effects model was chosen since intra-subject values are not independent from one another. The significance threshold was set at $P<0.05$.

RESULTS

Data Set

A total of 202 subjects were enrolled in the ERASE study between June 2017 and October 2019. Two subjects were excluded (1 had undergone carotid or vertebrobasilar intervention and another was claustrophobic and did not undergo MRI) yielding 200 subjects with MRI to be included in our study. Nine of these 200 subjects were excluded because of incomplete MRI data sets, partly because of claustrophobia. Of the 144 subjects with MRI scanned until February 2019 (with single C7 acquisition for both sides) 67 subjects were excluded as none of the carotid and basilar arteries met all quality criteria formulated in the Methods for the 2D PC acquisitions. Of the 56 subjects included after February 2019 only 6 subjects were excluded for not meeting all quality criteria. Thus 118 subjects were included, of whom 205 vessels were analyzed: 100 right ICA, 71 left ICA, and 34 BA. The baseline characteristics of the participants are shown in Table 1. Mean age was 46.2 years (SD±13; range, 20–70), 50 (42%) were men, 29 (25%) were current smokers, and 22 (19%) had hypertension.

Hemodynamic Measurements

Table 2 shows the hemodynamic parameters (blood-flow velocity, mean flow, and lumen area). The mean velocity and mean lumen area showed no difference from extracranial C1 to carotid canal C3. From carotid canal C3 to intracranial C7, across the carotid siphon, both mean and maximum velocities increased and mean lumen area decreased (all $P<0.001$). The mean flow decreased by 0.12±0.07 mL/s between C3 and C7. In contrast, a slight but significant area increase was seen from the C3 to C7 segment for the BA ($P<0.026$).

Pulsatility and Distensibility Along the ICA

The vPIs (pulsatility) and aPIs (distensibility) for extracranial—intracranial segments of the ICA are shown in Table 2 and visualized in Figure 3. An increase was found in vPI for both ICAs from the extracranial C1 up to the C3 segment in the carotid canal ($P<0.001$), which

Table 1. Baseline Characteristics of the 118 Subjects

Clinical Features	N=118 (114 White)
Age, y (range)	46.2±13 (20–70)
Men (%)/women (%)	50 (42)/68 (58)
BMI, kg/m²	26.2±4.1
Current smoker (%)	29 (25)
Systolic BP/diastolic BP, mm Hg	134±19/82.2±11
Ischemic stroke or TIA (%)	4 (3)
Myocardial infarction/intervention (%)	5 (4)
Diabetes mellitus (%)	7 (6)
Hypertension (men [%]/women [%])	22 (11 (9)/11 (9)
Hypercholesterolemia (%)	17 (14)

BMI indicates body mass index; BP, blood pressure; and TIA, transient ischemic attack.

Table 2. Schematic Overview of Hemodynamic Parameters and Velocity Pulsatility Index, Area Pulsatility Index and Flow Pulsatility Index for Every Vessel Per Segment

Vessel	Segment	Mean Velocity (cm/s)	Mean Lumen Area (mm^2)	Mean Flow (mL/s)	Velocity PI	Area PI
Right ICA	C1	25±5.2	14.9±3.87	3.57±0.98	0.84±0.13	0.18±0.07
Right ICA	C3	25±6.9	14.9±4.38	3.50±0.96	0.93±0.13	0.11±0.03
Right ICA	C7	35±10	9.5±3.43	3.30±0.92	0.83±0.12	0.30±0.09
Left ICA	C1	26±5.9	14.9±3.69	3.69±0.86	0.85±0.13	0.18±0.06
Left ICA	C3	25±7.7	14.8±4.48	3.56±0.83	0.94±0.14	0.11±0.04
Left ICA	C7	35±10	9.3±3.58	3.29±0.84	0.85±0.13	0.32±0.09
BA	C3	32±7.1	7.2±1.79	2.26±0.54	0.82±0.14	0.18±0.10
BA	C7	31±7.2	8.1±2.48	2.20±0.55	0.83±0.14	0.27±0.11

BA indicates basilar artery; ICA, internal carotid artery; and PI, pulsatility index.

was followed by a decrease in vPI from the C3 segment up to the intracranial C7 segment (*P*<0.001). There was no net difference in vPI between the extracranial C1 and intracranial C7 segment in either right (*P*=0.237) or left ICA (*P*=0.296). In the BA no change was found in vPI between segment C3 and C7 (*P*=0.539), while an increase was seen in aPI (*P*<0.001). All results for the fPI measurements were similar to the vPI results and can be found in Table S1.

The trends across segments were inverse for aPI indices: where vPI increases between C1 and C3 and decreases again at C7; aPI decreases between C1 and C3, and subsequently increases again to C7. The observations were consistent for both ICAs: 168 out of 171 individual ICA vPI measurements (98%) and 162 out of 171 aPI measurements (95%) showed the same trend.

The vPIs and aPIs per segment and vessel categorized by sex are shown in Table 3. Significantly higher vPIs were found with increasing age (*P*<0.015) as well as in men compared with women for both ICAs at all 3 ICA segments (all *P*<0.001). This sex difference remained unchanged with increasing age. Although the attenuation of vPI over the carotid siphon decreased with increasing age (*P*=0.038) and the increase of vPI was the highest at C7 level, no significant change was seen over the whole ICA trajectory with increasing age (*P*=0.519) (Figure 4). In addition, no changes in distensibility were observed along the whole ICA trajectory for age (Figure 4). The vPI and aPI did not change with age for the BA.

DISCUSSION

In this study, we described variation in vPI and aPI over the whole ICA considering effects of age and sex. Overall there was no significant attenuation in
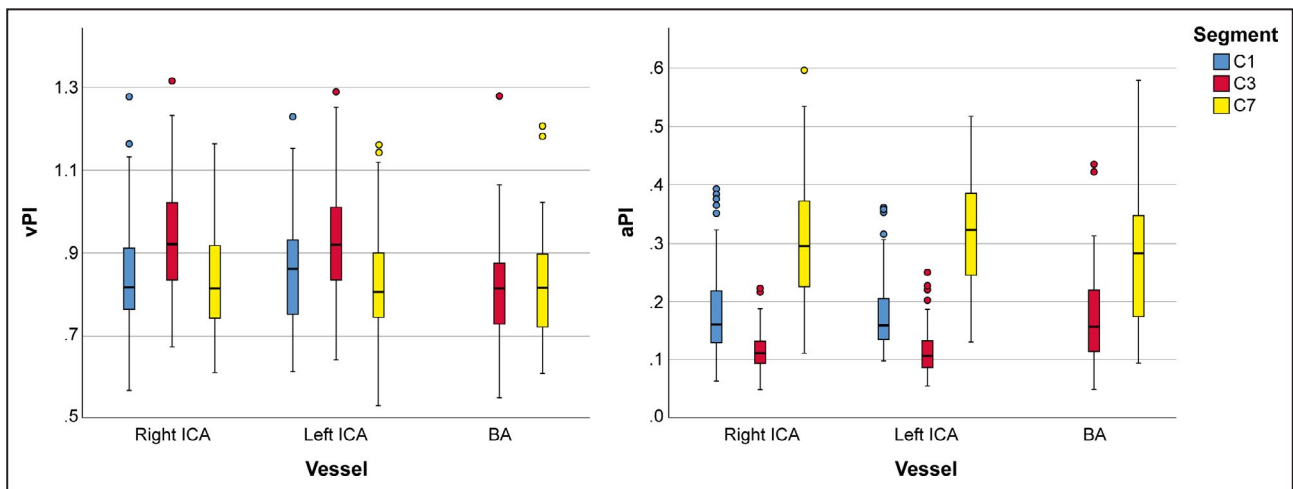

Figure 3. Velocity pulsatility index (left) and area pulsatility index (right) per vessel for each segment showing inverse trends across segments for the velocity pulsatility and area pulsatility indices.
The area pulsatility decreases between C1 and C3, and subsequently increases again to C7, the velocity pulsatility increases between C1 and C3 and decreases again at C7. aPI indicates area pulsatility index; BA, basilar artery; ICA, internal carotid artery; and vPI, velocity pulsatility index.

Table 3.   Velocity Pulsatility Index and Area Pulsatility Index (Mean Values±SD) Per Vessel and Segment for Both Men and Women

Vessel	Segment	Men vPI	Women vPI	*P* Value	Men aPI	Women aPI	*P* Value
Right ICA	C1	0.89±0.13	0.80±0.11	<0.001	0.18±0.07	0.18±0.06	0.37
Right ICA	C3	1.00±0.13	0.89±0.11	<0.001	0.11±0.04	0.12±0.03	0.69
Right ICA	C7	0.87±0.13	0.80±0.11	0.02	0.31±0.11	0.29±0.08	0.23
Left ICA	C1	0.90±0.13	0.81±0.11	0.005	0.16±0.05	0.19±0.05	0.06
Left ICA	C3	0.99±0.14	0.89±0.11	0.005	0.12±0.04	0.11±0.04	0.20
Left ICA	C7	0.89±0.15	0.79±0.09	0.01	0.34±0.10	0.31±0.08	0.13
BA	C3	0.84±0.17	0.81±0.13	0.31	0.22±0.12	0.17±0.09	0.06
BA	C7	0.84±0.18	0.82±0.11	0.58	0.28±0.12	0.26±0.10	0.75

aPI indicates area pulsatility index; BA, basilar artery; ICA, internal carotid artery; and vPI, velocity pulsatility index.

velocity pulsatility from extracranial C1 to intracranial C7, although we found an increase of velocity pulsatility between the extracranial (C1) part of the ICA and the carotid canal (C3) with a subsequent decrease
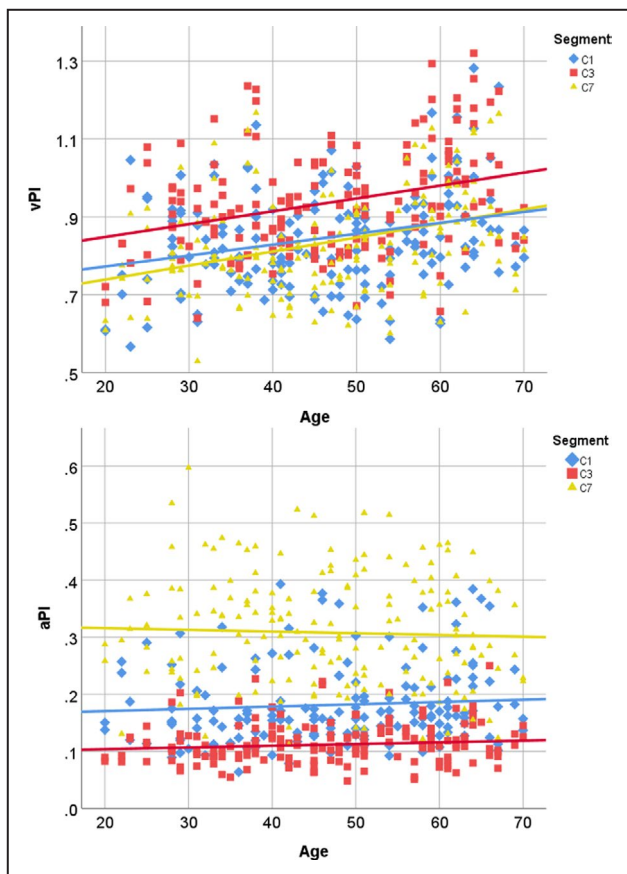
Figure 4.   The effect of age on both velocity pulsatility index (upper) and area pulsatility index (lower) across segments are illustrated using trend lines.
Velocity pulsatility index C1: y=0.0028x+0.7167, velocity pulsatility index C3: y=0.0033x+0.7824 and velocity pulsatility index C7=0.0036x+0.6671. For area pulsatility index C1: y=0.0004x+0.1623, area pulsatility index C3: y=0.0003x+0.0979 and area pulsatility index C7: y=−0.0003x+0.3218. aPI indicates area pulsatility index; and vPI, velocity pulsatility index.

between C3 and the intracranial (C7) part of the ICA. Conversely, where vPI increases between C1 and C3 and decreases again at C7, aPI decreases between C1 and C3, and subsequently increases again to C7. Men and women showed similar trends along the ICA, but the vPI in men was significantly higher compared with women at every segment. The lack of attenuation in velocity pulsatility between C1 and C7 did not change with age. At the same time, there was significantly less attenuation of vPI over the carotid siphon with increasing age.

The characteristic tortuous shape of the carotid siphon may be an explanation of attenuation of vPI and fPI. We confirmed previous studies showing attenuation of vPI over the carotid siphon (C3–C7 segment).[11,14] Although the BA is not an ideal control, the stability of vPI over the straight BA suggests that both the bony carotid canal and the tortuous shape of the carotid siphon may contribute to changes in pulsatility. The decrease over the siphon may be interpreted as a local restoring function rather than an effective decrease for the entire ICA, as we found an increase in the vPI and fPI between the extracranial C1 and the C3 segments. The limited ability for the ICA to expand at C3 segment, constrained by the rigid boundaries of the bony carotid canal, is probably the cause of the significant increase of vPI and fPI and decreased distensibility (aPI) compared with extracranial C1, surrounded by soft tissue, and intracranial C7, surrounded by cerebral spinal fluid.

We observed a positive association with vPI and age that was strongest at the C7 segment. Consequently we observed a decrease in vPI attenuation over the carotid siphon with increasing age as well. This is in line with progressive stiffening of the carotid siphon as a result of increasing calcification that is common with increasing age.[15] This stiffening process is probably influenced by hypertension which was present in 19% of our participants.[16,17] This study supports earlier observations that age is an important factor for increased arterial pulsatility.[18,19]

It is known that blood-flow velocities are higher in men than women at rest and that sex differences may contribute to lower incidence of cardiovascular disease in premenopausal women.[20] Distinct sex differences in the incidence and severity of hypertension are also well established, with men having a higher incidence of hypertension compared with women of the same age.[21–23] Our study confirms that hypertension is more frequent in the men (22% versus 16%) with a comparable mean age (men 47.4 years; women 45.3 years). The higher vPI values in men are in accordance with the higher blood pressure values at the same age.[24,25] We found a significant sex difference in vPI for every segment of the ICA. This observation is in accordance with a previous study, which showed higher pulsatility in men in 8 out of 11 different vessels, although this was not statistically significantly different for the individual vessels.[14] A difference with our study is that the ROIs were manually drawn and were of fixed size for the entire cardiac cycle, therefore no distensibility of the artery was considered. Active contour detection adapts the contours over the cardiac cycle, to capture the arterial distensibility. The thus additionally included low velocity values at the edge, may influence the velocity pulsatility and flow pulsatility. Based on the hemodynamic differences between sexes, a significant vPI difference is not unlikely, but needs to be studied in a larger population to further highlight the influence of sex differences on pulsatility.

Strengths of our study is that we used a larger and more representative population with a wide age range as compared with previous studies.[11,14] Moreover, we included the BA as a reference to ICA for variation in velocity pulsatility and arterial distensibility along a straight vessel segment. Besides, we separately assessed velocity and area pulsatilities rather than the flow pulsatility in which velocity and area effects join and potentially cancel out. The inclusion of an extracranial segment added new insights to the pulsatility along the ICA as well. The main limitation of our study is that many subjects had to be excluded as their flow measurements were inaccurate. Both right and left ICA flow measurements and the BA flow measurements were initially all performed simultaneously with a single 2D PC-MRI scan at 3 segments. Because of the diverging anatomy of intracranial ICA, this planning resulted in planes that were often not perfectly perpendicular to the vessels at C7 segment. The right and left ICA C7 segments should ideally have been planned separately, which was adapted in the protocol from February 2019 onwards, and greatly reduced the exclusion rates. The BA on C7 segment was no longer visible because of the angulation of the separate planned C7 segments, and therefore the number of included BA is limited. The strictly set inclusion and exclusion criteria resulted in a large drop out of included subjects, but enforced at the same time inclusion of only perpendicularly planned flow measurements. Two-dimensional PCA is a verified technique, and all ROIs were automatically created upon a single mouse click by the Philips scanner software without any manual correction that could influence the drawn region of interest. The automated region of interest selection was performed twice in 5 subjects and this did not change any measurements. The results also indicate repeatability of the results, as both right and left ICA, and the 2 BA levels showed similar vPI and aPI within the same patient. Moreover, the reported characteristic pattern along the ICA for both vPI and aPI was present in >95% of the individual subjects, indicating that we report a robust phenomenon that can be detected on an individual basis. A possible limitation is the relatively low temporal resolution of MRI compared with ultrasound, which could lead to underestimation of velocities. The underestimation of the velocities with MRI is expected to be independent of the location along the ICA, and does not affect the main findings of our study. Conversely, an important part of the ICA where it travels though the skull base is inaccessible for ultrasound. A further potential limitation is that the 2D PC-flow method we used may be less accurate than 4D PC-flow, which performs flow measurements in 3 directions over time.[26] However, 2D PC-MRI is a short acquisition with a high level of repeatability of volume flow changes in larger vessels such as the ICA.[27,28] Both methods have been shown to have similar measurement variability and equal measurement consistency.[29] The advantage of 4D flow measurements is that segments that are difficult to plan such as the diverging C7 segment can be reconstructed after scanning. However, 4D PC flow sequences acquired with submillimeter isotropic resolution often exceed 10 minutes scan time and have a relatively low temporal resolution.[30] The use of 4D PC-MRI in future studies could be beneficial for describing flow pulsatility and distensibility in the entire arterial tree simultaneously instead of separate slices and create a detailed vascular road map along the ICA.

CONCLUSIONS

We found similar decrease of pulsatility (vPI and fPI) over the carotid siphon as previous studies. However, the addition of distensibility and measurements at the extracranial and carotid canal segment of the ICA showed a more complex behavior than just decrease of pulsatility by the carotid siphon. The carotid siphon also has a restoring function for the pulsatility increase observed between the extracranial and carotid canal segment of the ICA. The bony carotid canal seems to constrain the distensibility of the ICA, thus increasing the pulsatility at carotid canal segment C3. Men have significantly higher vPI compared with women for all measured segments. Attenuation

of velocity pulsatility over the carotid siphon significantly decreases with aging, which is probably influenced by age and hypertension related stiffening of the carotid siphon. Future studies should focus on the influence of pathological processes, such as hypertension and vessel wall calcification, and on pulsatility and distensibility of the ICA.

ARTICLE INFORMATION

REFERENCES

1. James NL, Milijasevic Z, Ujhazy A, Edwards G, Jermyn K, Mynard JP, Celermajer DS. The common carotid artery provides significant pressure wave dampening in the young adult sheep. *Int J Cardiol Heart Vasc*. 2019;23:100343.

2. Humphrey JD, Na S. Elastodynamics and arterial wall stress. *Ann Biomed Eng*. 2002;30:509–523.

3. Gaballa MA, Jacob CT, Raya TE, Liu J, Simon B, Goldman S. Large artery remodeling during aging: biaxial passive and active stiffness. *Hypertension*. 1998;32:437–443.

4. O'Rourke MF, Hashimoto J. Mechanical factors in arterial aging: a clinical perspective. *J Am Coll Cardiol*. 2007;50:1–13.

5. Jagtap A, Gawande S, Sharma S. Biomarkers in vascular dementia: a recent update. *Biomarkers Genomic Med*. 2015;7:43–56.

6. Chang CW, Wai YY, Lim SN, Wu T. Association between flow acceleration in the carotid artery and intracranial aneurysms. *J Ultrasound Med*. 2019;38:1333–1340.

7. Ford MD, Alperin N, Lee SH, Holdsworth DW, Steinman DA. Characterization of volumetric flow rate waveforms in the normal internal carotid and vertebral arteries. *Physiol Meas*. 2005;26:477–488.

8. Hoi Y, Wasserman BA, Xie YJ, Najjar SS, Ferruci L, Lakatta EG, Gerstenblith G, Steinman DA. Characterization of volumetric flow rate waveforms at the carotid bifurcations of older adults. *Physiol Meas*. 2010;31:291–302.

9. Scheel P, Ruge C, Schoning M. Flow velocity and flow volume measurements in the extracranial carotid and vertebral arteries in healthy adults: reference data and the effects of age. *Ultrasound Med Biol*. 2000;26:1261–1266.

10. Roher AE, Garami Z, Tyas SL, Maarouf CL, Kokjohn TA, Belohlavek M, Vedders LJ, Connor D, Sabbagh MN, Beach TG, et al. Transcranial Doppler ultrasound blood flow velocity and pulsatility index as systemic indicators for alzheimer's disease. *Alzheimers Dement*. 2011;7:445–455.

11. Schubert T, Santini F, Stalder AF, Bock J, Meckel S, Bonati L, Markl M, Wetzel S. Dampening of blood-flow pulsatility along the carotid siphon: does form follow function? *AJNR Am J Neuroradiol*. 2011;32:1107–1112.

12. Bouthillier A, van Loveren HR, Keller JT. Segments of the internal carotid artery: a new classification. *Neurosurgery*. 1996;38:425–432.

13. Gosling RG, Dunbar G, King DH, Newman DL, Side CD, Woodcock JP, Fitzgerald DE, Keates JS, MacMillan D. The quantitative analysis of occlusive peripheral arterial disease by a non-intrusive ultrasonic technique. *Angiology*. 1971;22:52–55.

14. Zarrinkoob L, Ambarki K, Wahlin A, Birgander R, Carlberg B, Eklund A, Malm J. Aging alters the dampening of pulsatile blood flow in cerebral arteries. *J Cereb Blood Flow Metab*. 2016;36:1519–1527.

15. McClelland RL, Chung H, Detrano R, Post W, Kronmal RA. Distribution of coronary artery calcium by race, gender, and age: results from the Multi-Ethnic Study of Atherosclerosis (MESA). *Circulation*. 2006;113:30–37.

16. Savoia C, Burger D, Nishigaki N, Montezano A, Touyz RM. Angiotensin II and the vascular phenotype in hypertension. *Expert Rev Mol Med*. 2011;13:e11.

17. Chen NX, Moe SM. Vascular calcification: pathophysiology and risk factors. *Curr Hypertens Rep*. 2012;14:228–237.

18. Tarumi T, Khan MA, Liu J, Tseng BM, Parker R, Riley J, Tinajero C, Zhang R. Cerebral hemodynamics in normal aging: central artery stiffness, wave reflection, and pressure pulsatility. *J Cereb Blood Flow Metab*. 2014;34:971–978.

19. Xing C-Y, Tarumi T, Liu J, Zhang Y, Turner M, Riley J, Tinajero CD, Yuan L-J, Zhang R. Distribution of cardiac output to the brain across the adult lifespan. *J Cereb Blood Flow Metab*. 2017;37:2848–2856.

20. Sung BH, Vallabhan T, Wilson MF. Gender differences in brachial artery blood flow pattern at rest and during mental stress. *Psychosom Med*. 1999;61:113.

21. Gillis EE, Sullivan JC. Sex differences in hypertension: recent advances. *Hypertension*. 2016;68:1322–1327.

22. Mozaffarian D, Benjamin EJ, Go AS, Arnett DK, Blaha MJ, Cushman M, Das SR, de Ferranti S, Despres JP, Fullerton HJ, et al. Heart disease and stroke statistics-2016 update: a report from the American Heart Association. *Circulation*. 2016;133:e38–e360.

23. Yoon SS, Gu QP, Nwankwo T, Wright JD, Hong YL, Burt V. Trends in blood pressure among adults with hypertension united states, 2003 to 2012. *Hypertension*. 2015;65:54–61.

24. Khoury S, Yavows SA, O'Brien TK, Sowers JR. Ambulatory blood pressure monitoring in a nonacademic setting: effects of age and sex. *Am J Hypertens*. 1992;5:616–623.

25. Wiinberg N, Høegholm A, Christensen HR, Bang LE, Mikkelsen KL, Nielsen PE, Svendsen TL, Kampmann JP, Madsen NH, Bentzon MW. 24-h ambulatory blood pressure in 352 normal Danish subjects, related to age and gender*. *Am J Hypertens*. 1995;8:978–986.

26. Hsiao A, Alley MT, Massaband P, Herfkens RJ, Chan FP, Vasanawala SS. Improved cardiovascular flow quantification with time-resolved volumetric phase-contrast MRI. *Pediatr Radiol*. 2011;41:711–720.

27. Wåhlin A, Ambarki K, Hauksson J, Birgander R, Malm J, Eklund A. Phase contrast mri quantification of pulsatile volumes of brain arteries, veins, and cerebrospinal fluids compartments: repeatability and physiological interactions. *J Magn Reson Imaging*. 2012;35:1055–1062.

28. Schrauben E, Wahlin A, Ambarki K, Spaak E, Malm J, Wieben O, Eklund A. Fast 4D flow MRI intracranial segmentation and quantification in tortuous arteries. *J Magn Reson Imaging*. 2015;42:1458–1464.

29. Wåhlin A, Ambarki K, Birgander R, Wieben O, Johnson KM, Malm J, Eklund A. Measuring pulsatile flow in cerebral arteries using 4D phase-contrast MR imaging. *AJNR Am J Neuroradiol*. 2013;34:1740–1745.

30. van Ooij P, Zwanenburg JJM, Visser F, Majoie CB, vanBavel E, Hendrikse J, Nederveen AJ. Quantification and visualization of flow in the circle of willis: time-resolved three-dimensional phase contrast MRI at 7 T compared with 3 T. *Magn Reson Med*. 2013;69:868–876.

SUPPLEMENTAL MATERIAL

Table S1. Flow pulsatility index (mean values ± SD) per vessel and segment for men and women combined and separate, whereby the p-value illustrates the sex influence on fPI.

Vessel	Segment	Men fPI	Women fPI	p-value	Combined fPI
Right ICA	C1	0.96 ± 0.13	0.84 ± 0.11	<0.001	0.89 ± 0.13
Right ICA	C3	1.04 ± 0.13	0.92 ± 0.11	<0.001	0.97 ± 0.14
Right ICA	C7	0.92 ± 0.11	0.82 ± 0.11	0.001	0.87 ± 0.13
Left ICA	C1	0.90 ± 0.13	0.81 ± 0.12	<0.001	0.87 ± 0.14
Left ICA	C3	1.04 ± 0.17	0.89 ± 0.11	0.001	0.96 ± 0.16
Left ICA	C7	0.92 ± 0.16	0.78 ± 0.11	0.003	0.85 ± 0.15
BA	C3	0.94 ± 0.14	0.90 ± 0.15	0.31	0.92 ± 0.15
BA	C7	0.93 ± 0.12	0.82 ± 0.11	0.17	0.89 ± 0.14

fPI: flow Pulsatility Index; ICA: Internal Carotid Artery; BA: Basilar Artery.